XVI International Conference on Durability of Building Materials and Components
DBMC 2023, China
K.F. Li and D.P. Fang (Eds)

Study on Natural Passivation Behavior of Corrosion-resistant Steel Rebars in the Mortar

G. Liu[1*], D. Zhang[1,2,3*], H. Chen[1], Z. Fan[1,2,3], Q. Wu[3]

[1]Key Laboratory of Harbor & Marine Structure Durability Technology, Ministry of Transport, CCCC Fourth Harbor Engineering Institute Co., Ltd, Guangzhou 510230, PR China, lguoqiang5@cccc4.com (G. Liu), zhangdf8@mail.sysu.edu.cn (D. Zhang), chaoxiang@cccc4.com (H. Chen), fzhihong@cccc4.com (Z. Fan)

[2]Southern Marine Science and Engineering Guangdong Laboratory (Zhuhai), Zhuhai 519080, PR China, zhangdf8@mail.sysu.edu.cn (D. Zhang), fzhihong@cccc4.com (Z. Fan)

[3]National Observation and Research Station of Material Corrosion and Structural Safety of Hong Kong-Zhuhai-Macao Bridge in Guangdong, Zhuhai 519060, PR China, zhangdf8@mail.sysu.edu.cn (D. Zhang), fzhihong@cccc4.com (Z. Fan), wqf@hzmbo.com (Q. Wu)

Abstract. *The passivation behavior of HRB400 carbon steel rebar, 304 austenitic stainless steel rebar and 2304 austenitic-ferritic duplex stainless steel rebar during curing stage of mortar was studied by electrochemical testing techniques such as open-circuit potential, electrochemical impedance spectroscopy and linear polarization curve, and the corrosion resistance of the passivation film of the three rebars was compared to provide a reference for the practical engineering application of corrosion-resistant steel rebars. The study shows that all three types of steel rebars can be passivated during the 28 days curing stage of mortar, and 2304 duplex stainless steel rebars have the best passivation film corrosion resistance, followed by 304 stainless steel rebars, and HRB400 steel rebar was the worst.*

Keywords: *Corrosion-resistant rebars, Natural passivation behavior, Mortar.*

1 Introduction

Reinforced concrete is so widely used that it has become the most basic materials for infrastructure in transports, such as cross-sea bridges, operating platforms, port terminals, immersed tube tunnels, etc. However, due to the harsh service environment in marine, the reinforced concrete structures suffered serious corrosion under the long-term penetration of chloride and cause premature structural failure, which brings a series of economic, safety, and environmental problems (Melchers and Li 2009). It was well known that the main factors causing the failure of marine concrete structures is reinforcement corrosion (Ahmad 2003, Berke et al. 1992, Moser et al. 2012). During the early stage of cement hydration, the steel reinforcement generates a relatively dense passivation film on the interface of the concrete/steel in the high alkali condition, which can prevent corrosion to a certain extent. However, the presence of a large amount of the Cl^- both in the concrete materials and external environment can cause serious damage to the passivation film (Angst et al. 2009, Schueremans et al. 1999). Due to the denser passivation film on the surface of corrosion-resistant steel rebars and their excellent resistance to chloride and salt attack, the use of corrosion-resistant steel rebars to replace carbon steel rebars is one of the important way to release the corrosion risk of steel rebars and extend their service life (Bertolini et al. 1996, Castro et al. 2003, Baddoo 2008, Perez-Quiroz et al. 2008). 304 austenitic stainless steel rebar and 2304 austenitic-ferritic duplex stainless steel rebar have been applicated in some marine infrastructures due to their high resistance to corrosion media and low whole-life cost (Aldaca, et al. 2020, Padhy et al. 2011). A large amount of work has been performed to investigate the passivation behaviors of these stainless steel rebars in concrete simulating solution (Barbosa et al. 1991, Ogunsanya and Hansson 2019, Xya et al. 2020, Yuan et al. 2020), but the concrete pore simulation solution is not the same as the actual environment in which the reinforcement is placed, which has brought some hindrance to the practical application of corrosion-resistant steel rebars. Therefore, it is necessary to carry out research on the passivation behavior of different corrosion-resistant steel rebars in solid structures to provide better guidance for engineering applications.

In this work, the natural passivation behaviors of 304 stainless steel rebar and 2304 duplex stainless steel rebar were studied, and HRB400 carbon steel rebar was cast in mortar as a reference, and the passivation behavior during the curing stage was investigated by using open circuit potential, electrochemical impedance spectroscopy and linear polarization curves. The results will provide a guidance for the application of corrosion-resistant rebar for marine structures.

2 Experimental

The experimental materials were HRB400 carbon steel rebar, 304 stainless steel rebar, 2304 duplex stainless steel rebar with the composition were shown in Table 1. The above rebars were cut into Φ2 cm×2 cm (exposed area of 3.14 cm^2), and the end was welded with copper line and sealed with epoxy resin, and after curing, the bars were sealed with 40#, 100#, 360#, 600#, 1000#, 2000# sandpaper step by step, and rinsed and blown dry with ethanol and deionized water. The prepared rebar samples were poured with mortar in a 100 mm×100 mm×100 mm mold with a cover thickness of 2 cm, and the configuration table of mortar was shown in Table 2. Among them, cement for ordinary Portland cement, sand for standard sand. The mortar was placed in calcium hydroxide solution for curing stage and electrochemical testing. The electrochemical testing facility was Princeton 2273.

Table 1. The main components of the three types of steel rebar

	C	Si	Mn	P	S	N	Cr	Ni	Mo	Cu
HRB400	0.25	0.80	1.60	0.045	0.045	-	-	-	-	-
304	0.07	1.00	2.00	0.045	0.015	0.11	17.5~19.5	8.0~10.5	-	-
2304	0.03	1.00	2.00	0.035	0.015	0.05~0.20	22.0~24.0	3.5~5.5	0.10~0.60	0.10~0.60

Table 2. The proportion of mortar(kg/m^3)

Samples	Cement	Sand	Water
Mortar	450	1350	225

The open circuit potential, electrochemical impedance spectroscopy and linear polarization curve were tested daily during the curing period of the reinforced mortar system last for 28 days. The frequency range of the electrochemical impedance spectrum test was 100 kHz to 10 mHz with an amplitude of 10 mV, and the data were analyzed using ZSimp Win software for a reasonable equivalent circuit fit. The linear polarization curve test polarizes the relative corrosion potential E_{corr}=±20 mV of the steel rebar with a scan rate of 3 mV/s. After fitting, the polarization resistance R_p of the steel rebar can be obtained, and the corrosion current density i_{corr} of the steel bar can be found by the Sten-Geary formula ($i_{corr}=B/R_p$) where B is the Tafel constant, when the rebar is in the blunt state, generally take the value of 52 mV (Law et al. 2000).

3 Results and Discussion

Figure 1 showed the open circuit potential versus time for HRB400 plain rebar, 304 stainless steel rebar and 2304 duplex stainless steel rebar mortar system at different ages. The open-circuit potential of all three types of rebar increased with age and grew more rapidly before 7 d. The open-circuit potential of HRB400 plain rebar grew slowly to -210.85 mV during the age of 7 d~28 d, while the open-circuit potential of 304 stainless steel rebar and 2304 duplex stainless steel rebar in mortar still grew faster to -110.58 mV and -116.61 mV. This indicated that the surfaces of the three rebar types stabilized during the mortar oxidation process and were in a passivated state within 28 d.

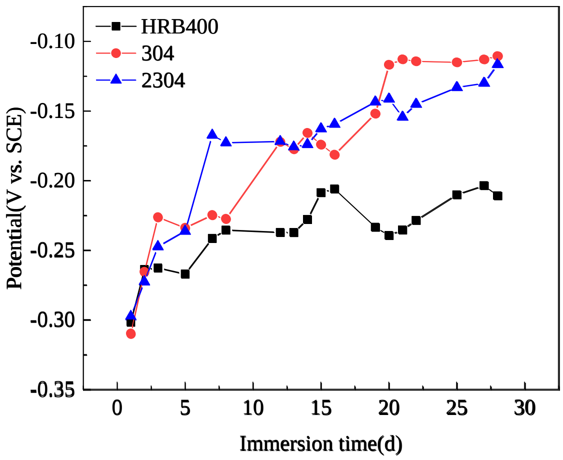

Figure 1. Variation of open circuit potential with age for three types of rebar during curing stage of mortar.

The electrochemical impedance spectroscopy of the three rebar mortar systems were tested at different ages, and the results are shown in Figure 2. It can be seen from the figure that the radius of capacitive arc resistance, low-frequency impedance modulus, and phase angle peak width of the three rebar systems showed a trend of gradual increase as the age increased, and the maximum phase angle moved toward the low frequency. After 28 d of curing, the radius of capacitive arc resistance and low-frequency impedance modulus of 2304 duplex stainless steel rebar were larger than those of 304 stainless steel rebar, and HRB400 plain rebar was the smallest.

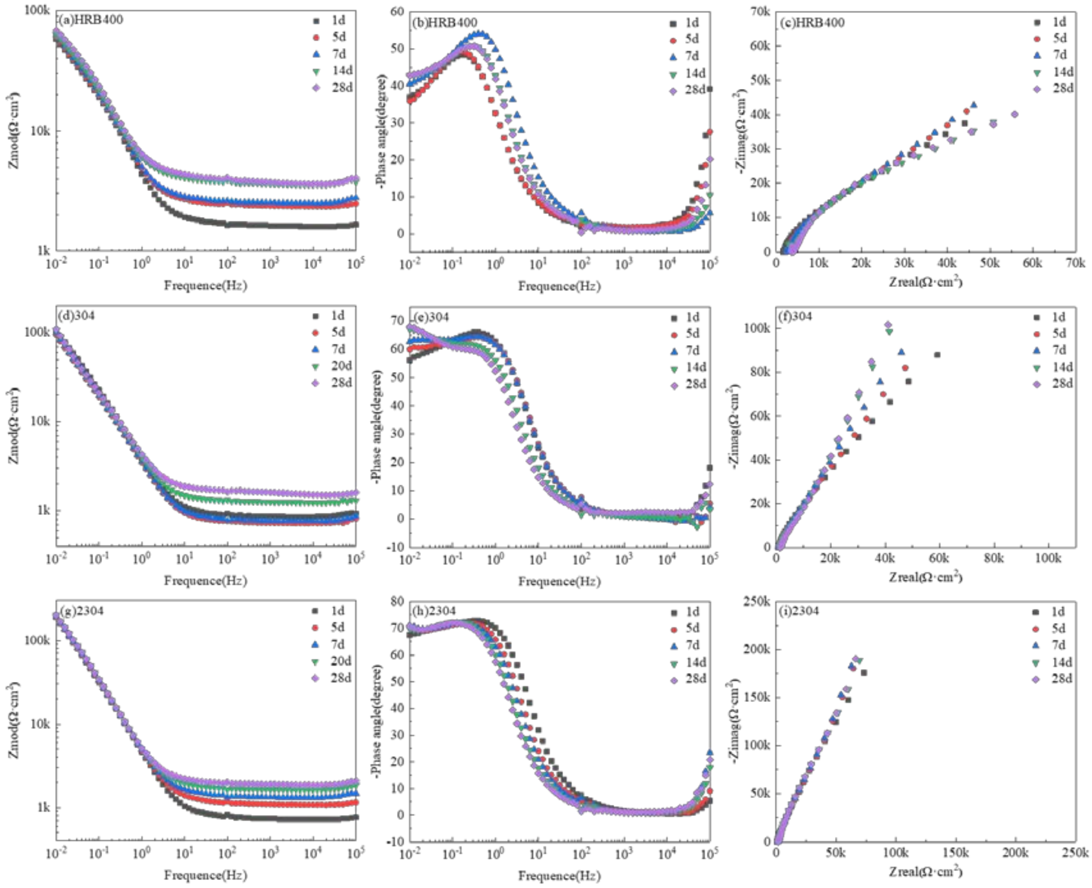

Figure 2. Electrochemical impedance spectroscopy of three types of rebar during curing stage of mortar: (a), (b) Bode plot, (c) Nyquist plot for HRB400 plain rebar; (d), (e) Bode plot, (f) Nyquist plot for 304 stainless steel rebar; (g), (h) Bode plot, (i) Nyquist plot for 2304 duplex stainless steel rebar.

The Bode plots of the three types of rebar show that the phase angles in the low frequency range exhibit asymmetry, indicating the existence of two overlapping time constants (Xya et al. 2020); moreover, the maximum phase angle in the Bode plots is less than 90°. Based on the results and analysis of the electrochemical impedance spectroscopy, the data were fitted using the equivalent circuit of Figure 3 (Zheng et al. 2020), considering the redox reaction on the surface of the rebar (Shi et al. 2020). Where, R_o is the mortar resistance, R_{ct} is the charge transfer resistance, Q_{dl} is the double layer capacitance, R_f is the passivation film resistance, and Q_f is the passivation film capacitance.

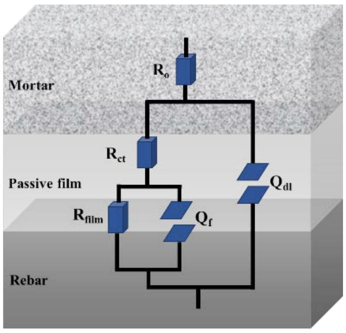

Figure 3. Equivalent circuit diagram used for rebars during curing stage of mortar.

The fitting parameters for electrochemical impedance spectroscopy of the three rebar mortar systems at different ages were shown in Table 3. The variation of charge transfer resistance R_{ct} with age and the variation of resistance R_f of passivation film with age shown in figure 4. The R_{ct} of both HRB400 plain rebar and 304 stainless steel rebar grew slowly during the 28 d curing process, while 2304 duplex stainless steel rebar grew rapidly during the ages of 1 d~7 d and slowly at the later stages. The R_f of all three types of rebar increased with age, and the passivation film layer resistance R_f of HRB400 plain rebar, 304 stainless steel rebar and 2304 duplex stainless steel rebar reached 0.26 MΩ, 1.51 MΩ and 2.69 MΩ after 28 d of curing, respectively. It is better than 304 stainless steel rebar and better than HRB400 plain rebar.

Table 3. Fitting parameters for electrochemical impedance spectroscopy of the three rebar mortar systems at different ages.

Rebar-Mortar	Time	R_0 ($\times10^3\Omega\cdot cm^2$)	Q_0-Y_0 ($\times10^{-5}\Omega^{-1}\cdot cm^{-2}\cdot s^n$)	Q_0-Y_n	R_{ct} ($\times10^4\Omega\cdot cm^2$)	Q_{dl}-Y0 ($\times10^{-5}\Omega^{-1}\cdot cm^{-2}\cdot s^n$)	Q_{dl}-Y_n	R_f ($\times10^5\Omega\cdot cm^2$)	Chi-squared ($\times10^{-3}$)
HRB400	1D	1.63	6.06	0.81	4.21	14.92	0.78	1.23	0.63
	5D	2.40	6.15	0.81	4.48	13.46	0.76	1.74	0.95
	7D	2.56	6.05	0.81	4.59	12.73	0.76	1.78	2.21
	14D	3.70	6.12	0.79	4.83	7.57	0.51	1.95	8.26
	28D	3.83	5.88	0.77	5.22	4.01	0.32	2.63	5.30
304	1D	0.88	5.60	0.86	6.52	3.72	0.68	6.68	1.70
	5D	0.74	6.64	0.84	6.72	4.52	0.78	6.81	0.49
	7D	0.78	6.46	0.84	6.75	4.18	0.82	6.94	0.42
	14D	1.26	6.28	0.83	8.57	4.22	0.91	10.98	0.68
	28D	1.60	6.21	0.82	9.84	3.78	0.94	15.07	2.20
2304	1D	0.75	4.22	0.89	8.19	1.18	0.74	8.28	1.24
	5D	1.11	4.48	0.87	34.35	2.58	1.00	12.79	0.96
	7D	1.30	4.45	0.86	36.79	2.13	0.98	15.56	4.52
	14D	1.89	4.35	0.90	37.12	3.21	1.00	18.61	9.85
	28D	1.93	4.44	0.87	56.49	2.61	1.00	26.91	2.95

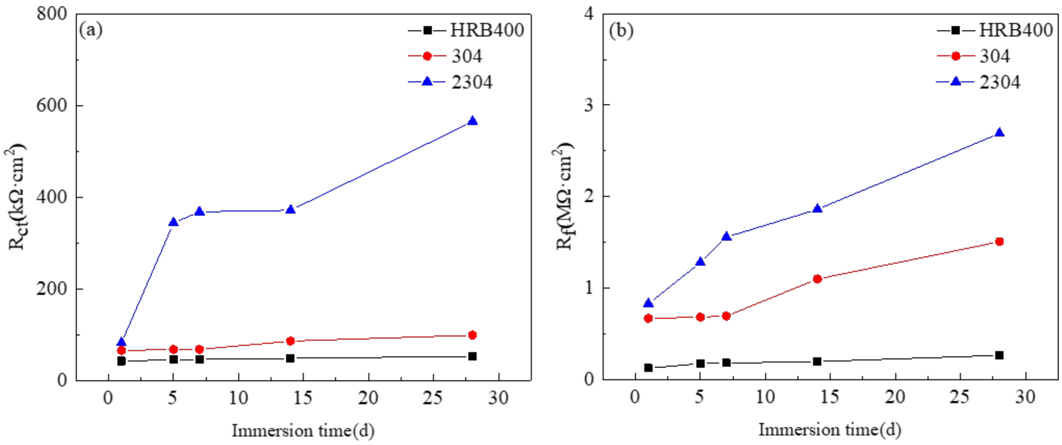

Figure 4. Fitting results of electrochemical impedance spectroscopy of three types of rebar during curing stage of mortar: (a) Variation of charge transfer resistance R_{ct} with age; (b) Variation of resistance R_f of passivation film with age.

The polarization curves were tested for three types of rebar mortars at different ages, and the results are shown in Figure 5. With the growth of age, the linear polarization curves shifted negatively along the X-axis and positively along the Y-axis, i.e., the corrosion potential kept increasing and the corrosion current density kept decreasing, which indicated that the rust probability and corrosion rate of rebar gradually decreased, i.e., the three types of rebar gradually passivated during curing stage of mortar and the surface passivation film gradually stabilized. The results of the linear polarization curves were fitted and the results are shown in Figure 6. With the growth of age, the corrosion current density of the three types of rebar in mortar all showed different degrees of decrease, and after 28 d of curing, the corrosion current density of HRB400 rebar, 304 stainless steel rebar and 2304 duplex stainless steel rebar were 0.492 μA/cm^2, 0.237 μA/cm^2, 0.171 μA/cm^2 respectively, which indicated that during 28 d of curing, 2304 duplex stainless steel rebar passivated best, followed by 304 stainless steel rebar, HRB400 rebar was the worst.

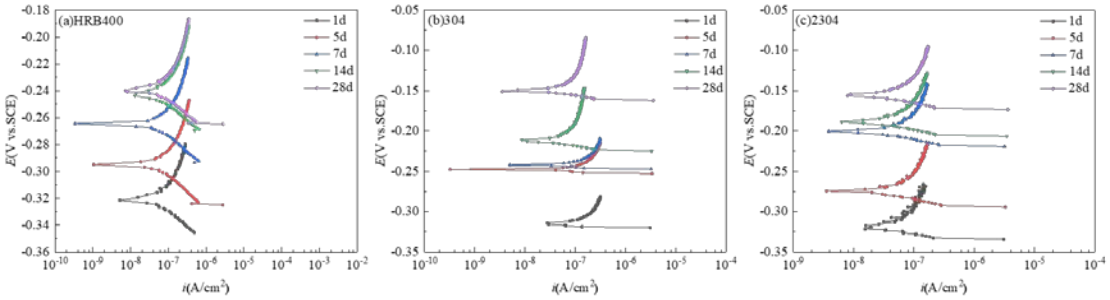

Figure 5. Linear polarization curves of three types of rebar at different ages during curing stage of mortar.

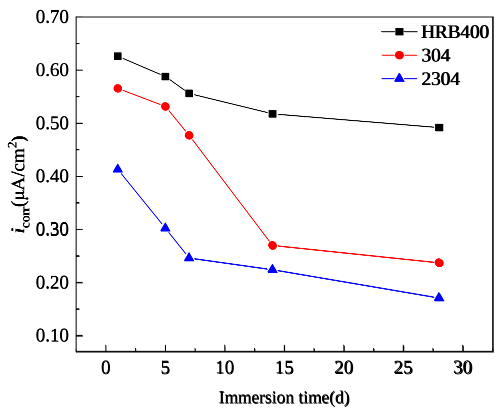

Figure 6. Corrosion current density of three types of rebar at different ages during curing stage of mortar.

4 Conclusion

- The electrochemical test indicated that, HRB400 rebar, 304 stainless steel rebar and 2304 duplex stainless steel rebar all complete passivation during the 28 d curing of mortar. HRB400 rebar passivates faster in 1~7 d of mortar curing and more slowly in the later period. 304 and 2304 stainless steel rebar grows rapidly in 1~14 d of surface passivation film and also passivates faster in the later period of mortar curing.
- 2304 duplex stainless steel rebar has the best corrosion resistance of surface passivation film after cement hydration, and the film resistance is 1.5 times that of 304 stainless steel rebar and 10.2 times that of HRB400 plain steel rebar.

Acknowledgements

We acknowledge the support from the National Key Research and Development Program of China (No. 2019YFB1600700)

References

Ahmad, S. (2003). *Reinforcement corrosion in concrete structures, its monitoring and service life prediction-a review*. Cement Concrete Composites, 25(4-5), 459-471.

Aldaca, I., Briz, E., Garcia, H., and Corro, A.M. (2020). *The Weldability of Duplex Stainless-Steel in Structural Components to Withstand Corrosive Marine Environments*. Metals, 10, 1-24.

Angst, U., Elsener, B., and Larsen, C.K. (2009). *Critical chloride content in reinforced concrete-A review*. Cement concrete research, 39(12), 1122-1138.

Berke, N.S., and Hicks, M.C. (1992). *Estimating the life cycle of reinforced concrete decks and marine piles using laboratory diffusion and corrosion data*.

Bertolini, L., Bolzoni, F., Pastore, T., and Pedeferri, P. (1996). *Behaviour of stainless steel in simulated concrete pore solution*. British Corrosion Journal, 31(3), 218-222.

Castro, H., Rodriguez, C., Belzunce, F.J., and Canteli, A.F. (2003). *Mechanical properties and corrosion behaviour of stainless steel reinforcing bars*. Journal of Materials Processing Technology, 143–144(1), 134-137.

Law, D.W., Millard, S.G., and Bungey, J.H. (2000). *Linear polarisation resistance measurements using a potentiostatically controlled guard ring*. NDT&E International, 33, 15-21.

Barbosa, M.A., Garrido, A., Campilho, A., Sutherland, I. (1991). *The surface composition and corrosion behaviour of AISI 304 stainless steel after immersion in 20% HNO_3 solution*. Corrosion Science, 32(2), 179-184.

Melchers, R.E., and Li, C.Q. (2009). *Reinforcement corrosion initiation and activation times in concrete structures exposed to severe marine environments*. Cement concrete research, 39(11), 1068-1076.

Moser, R.D., Singh, P.M., Kahn, L.F., and Kurtis, K.E. (2012). *Chloride-induced corrosion resistance of high-strength stainless steels in simulated alkaline and carbonated concrete pore solutions*. Corrosion Science, 57, 241-253.

Baddoo., N.R. (2008). *Stainless steel in construction: A review of research, applications, challenges and opportunities.* Journal of Constructional Steel Research, 64(11), 1199-1206.

Ogunsanya, I.G., and Hansson, C.M. (2019). *The semiconductor properties of passive films and corrosion behavior of stainless steel reinforcing bars in simulated concrete pore solution*. Materialia, 6, 100321.

Padhy, N., Paul, R., Mudali, U. K., and Raj, B. (2011). *Morphological and compositional analysis of passive film on austenitic stainless steel in nitric acid medium*. Applied Surface Science, 257(11), 5088-5097.

Perez-Quiroz, J.T., Teran, J., Herrera, M.J., Martinez, M., and Genesca, J. (2008). *Assessment of stainless steel reinforcement for concrete structures rehabilitation*. Journal of Constructional Steel Research, 64(11), 1317-1324.

Schueremans, Van, and Gemert. (1999). *Service life prediction of reinforced concrete structures, based on in-service chloride penetration profiles*. Paper presented at the 8th INTERNATIONAL CONFERENCE ON DURABILITY OF BUILDING MATERIALS AND COMPONENTS, Vancouver, Canada.

Shi, J., Ming, J., and Wu, M. (2020). *Passivation and corrosion behavior of 2304 duplex stainless steel in alkali-activated slag materials*. Cement Concrete Composites, 108, 103532.

Xya, B., Xuan, W., Yang, C., and Hy, A. (2020). *Natural passivation behavior and its influence on chloride-induced corrosion resistance of stainless steel in simulated concrete pore solution*. Journal of Materials Research and Technology, 9(6), 12378-12390.

Yuan, X., Li, W., Wang, X., and Yang, H. (2020). *Mo Effect on Natural Passivation and Corrosion Behavior of Duplex Stainless Steels in Alkaline Media*. Journal of the Electrochemical Society, 167(16), 161509.

Zheng, H., Dai, J. G., Hou, L., Meng, G., and Li, W. (2020). *Enhanced passivation of galvanized steel bars in nano-silica modified cement mortars*. Cement Concrete Composites, 111, 103626.